On the Jones-Wilkins-Lee equation of state for high explosive products

Gabriel Farag, Ashwin Chinnayya

▶ **To cite this version:**

Gabriel Farag, Ashwin Chinnayya. On the Jones-Wilkins-Lee equation of state for high explosive products. Propellants, Explosives, Pyrotechnics, 2024, 49 (3), 10.1002/prep.202300223 . hal-04519251

HAL Id: hal-04519251
https://hal.science/hal-04519251

Submitted on 25 Mar 2024

HAL is a multi-disciplinary open access archive for the deposit and dissemination of scientific research documents, whether they are published or not. The documents may come from teaching and research institutions in France or abroad, or from public or private research centers.

L'archive ouverte pluridisciplinaire **HAL**, est destinée au dépôt et à la diffusion de documents scientifiques de niveau recherche, publiés ou non, émanant des établissements d'enseignement et de recherche français ou étrangers, des laboratoires publics ou privés.

On the Jones-Wilkins-Lee equation of state for high explosive products

Gabriel Farag, Ashwin Chinnayya

[a]*Institut Pprime UPR CNRS 3346 ISAE-ENSMA UniversitÃl' de Poitiers 86961 Futuroscope-Chasseneuil Cedex France*

https://doi.org/10.1002/prep.202300223

Abstract

The Jones-Wilkins-Lee (JWL) model is a widely used Equation Of State (EOS) in the literature to model high explosive products. It is based on exponentially decaying isentropes in the pressure-volume diagram, completed by an additional term meant to recover an ideal-gas behavior for large expansions where exponential terms are negligible. A step-by-step analysis of the EOS is proposed. Starting from the main isentrope, the constant Grüneisen, and constant isochoric heat capacity, the JWL expressions of pressure, temperature, sound speed, specific internal energy, specific entropy and specific enthalpy are derived. For a specific set of JWL parameters meant to model HMX products, various thermodynamic fields are investigated in pressure–volume and temperature–volume planes. The positivity of pressure and temperature, the convexity, the thermodynamic stability, and the monotonicity along an Hugoniot are investigated in order to characterize the JWL domain of validity. For each of these constraints, different regions of validity are found. Besides presenting a study of the JWL model and its limits, this work also provides a standalone presentation and derivation containing the necessary materials for the understanding and for the use of the JWL EOS in reactive hydrodynamic simulations of condensed phase explosives.

Keywords: Jones-Wilkins-Lee; detonation; condensed explosive; high explosive; product equation of state

Email addresses: gabriel.farag@ensma.fr (Gabriel Farag), ashwin.chinnayya@ensma.fr (Ashwin Chinnayya)

Nomenclature

p	Pressure	Pa
v	Specific volume	$\mathrm{m}^3 \cdot \mathrm{kg}^{-1}$
s	Entropy	$\mathrm{J} \cdot \mathrm{kg}^{-1} \cdot \mathrm{K}^{-1}$
e	Internal energy	$\mathrm{J} \cdot \mathrm{kg}^{-1}$
h	Enthalpy	$\mathrm{J} \cdot \mathrm{kg}^{-1}$
T	Temperature	K
c	Sound speed	$\mathrm{m} \cdot \mathrm{s}^{-1}$
Γ	Grüneisen coefficient	
C_v	Specific heat capacity at constant volume	$\mathrm{J} \cdot \mathrm{kg}^{-1} \cdot \mathrm{K}^{-1}$
s_{ref}	Entropy of the reference isentrope	$\mathrm{J} \cdot \mathrm{kg}^{-1} \cdot \mathrm{K}^{-1}$
p_{ref}	Pressure of the reference isentrope	Pa
e_{ref}	Internal energy of the reference isentrope	$\mathrm{J} \cdot \mathrm{kg}^{-1}$
v_0	Specific volume of unreacted explosive	$\mathrm{m}^3 \cdot \mathrm{kg}^{-1}$
p_{CJ}	Chapman-Jouguet pressure	Pa
v_{CJ}	Chapman-Jouguet specific volume	$\mathrm{m}^3 \cdot \mathrm{kg}^{-1}$
e_{CJ}	Chapman-Jouguet internal energy	$\mathrm{J} \cdot \mathrm{kg}^{-1}$
D_{CJ}	Chapman-Jouguet velocity	$\mathrm{m} \cdot \mathrm{s}^{-1}$
T_{CJ}	Chapman-Jouguet temperature	K
q	Chapman-Jouguet heat release	$\mathrm{J} \cdot \mathrm{kg}^{-1}$

1. Introduction

During any event of transition to detonation of a condensed phase explosive, the leading shock wave increases the pressure and the temperature, and therefore triggers the chemical reactions in the explosive. Heat exchanges can occur between the unreacted material and the products in the reaction zone. The modeling of the products is therefore important, as it governs the partition between the kinetic and internal energies. Moreover, the expansion of the products can be used to propel surrounding materials [1–4].

When a thorough understanding of a physical phenomenon is not readily available, it is often difficult to derive a complete and meaningful model taking into account all relevant physical processes. A simplified model with calibrated parameters can be used to reproduce certain physical phenomena for engineering applications. As for the modeling of condensed phase detonation products, the Jones-Wilkins-Lee (JWL) equation of state (EOS) belongs to the latter category. Its first published mention can be traced back to the contributions of [5] and [6], which have been notably inspired by the works of [7] and [8].

More refined EOS can also be found in the condensed phase explosive literature including *e.g.*, the H9 ([9]) and the well known Becker-Kistiakowsky-Wilson ([10, 11]) models. Nonetheless, due to its simplicity, the JWL model is among the most widely used EOS for the high explosive products modeling, see *e.g.*, Refs.[2, 12–15]. It requires a careful calibration of various adjustable parameters in order to fit experimental or theoretical results see *e.g.*, [16–20]. Being widely used in the literature it is surprising to mention that very few sources actually address the derivation and study of the JWL model itself from a thermodynamic standpoint, possibly due to its composite and empirical origin. Some important milestones of the JWL analysis can be found in [21], [22], [23], and [20]. Nonetheless a step-by-step derivation and dedicated investigation of JWL thermodynamics and domain of validity is still lacking.

Therefore the purpose of the present work is twofold. First, a thermodynamically consistent derivation of various forms of the JWL EOS from the isentropes is provided. More specifically, the expressions of the pressure, specific internal energy, sound speed, temperature, specific enthalpy, and specific entropy are derived, allowing the use of the JWL model in reactive hydrodynamic problems. Second, the model calibrated to HMX products is discussed and its domain of validity with regard to various thermodynamic constraints

is investigated and discussed.

With a view to simplification, the presentation is organized as follows. Section 2 presents the JWL isentropes along with pressure–volume–entropy and internal energy–volume–entropy forms. In Sect. 3, by using the assumption of a constant Grüneisen, the sound speed and pressure–internal energy–volume forms are derived, and the JWL model is expressed in a Mie-Grüneisen form. In Sect. 4, thermal and caloric expressions of temperature, specific enthalpy, and specific entropy are derived. Then, Sect. 5 is devoted to the qualitative analysis of the model for some HMX parameters. In Sect. 6, the domain of validity of positive temperature, positive pressure, convexity, thermodynamic stability and monotonicity along the Hugoniot curve are investigated. Finally, conclusions are drawn in Sect. 7.

2. The Jones-Wilkins-Lee isentropes

The pedestrian derivation leading to a JWL model, which is to be implemented into a hydrodynamic code, starts by the early stages of the demonstration proposed by [23]. The $p(v, s)$ isentropes selected in the JWL model read as,

$$p(v,s) = A\exp\left(-R_1\frac{v}{v_0}\right) + B\exp\left(-R_2\frac{v}{v_0}\right) + C(s)\left(\frac{v}{v_0}\right)^{-(\Gamma+1)}, \tag{1}$$

where v and v_0 denote the current and initial specific volume of the material, p is the thermodynamic pressure, s the entropy, and Γ the Grüneisen coefficient that is assumed constant in the classical JWL model. When the JWL EOS is used for detonation products, A, B, R_1, and R_2 are the remaining positive parameters, which need to be fitted to reference sets of data.

This particular form of isentropes has been selected from empirical comparisons decades ago. It was also recently revisited in the work of [21] by using the universal curve of [24] (p/p_{CJ} as a function of u/u_{CJ} along the isentrope issued from the CJ state) and the tangency of Crussard and isentrope curves in the vicinity of CJ point in the p–v diagram. [20] showed how to derive the different parameters from only the detonation velocity and the initial density, from the compilation of empirical data and correlations. The JWL various terms can therefore be interpreted as follows.

- The first term proportional to A is meant to model high pressure expansions close to CJ state.
- The second term proportional to B is meant to model intermediate pressure expansions.
- The third term scaling proportional to C is meant to model an ideal-gas behavior appearing at low pressures and large expansions.

According to [8], the function $C(s)$ only depends on entropy, which is yet to be specified but should not be a constant function to avoid Eq. (1) to degenerate into a barotropic EOS.

Among this family of isentropes, an arbitrary reference entropy s_{ref} is selected corresponding to the isentrope curve $p_{\text{ref}}(v) = p(v, s_{\text{ref}})$. It can be expressed by,

$$p_{\text{ref}}(v) = A \exp\left(-R_1 \frac{v}{v_0}\right) + B \exp\left(-R_2 \frac{v}{v_0}\right) + C^* \left(\frac{v}{v_0}\right)^{-(\Gamma+1)}, \tag{2}$$

where $C^* = C(s_{\text{ref}})$ is a constant. In this article, $p_{\text{ref}}(v)$ will be referred to as the main isentrope. Then, using Eqs. (1,2), the $p(v, s)$, EOS could be recast in a more compact equation in term of the reference isentrope curve $p_{\text{ref}}(v)$,

$$p(v, s) = p_{\text{ref}}(v) + (C(s) - C^*) \left(\frac{v}{v_0}\right)^{-(\Gamma+1)}. \tag{3}$$

Now, from thermodynamic relations [25], the pressure can be related to the specific internal energy, entropy, and volume by

$$p = -\left(\frac{\partial e}{\partial v}\right)_s. \tag{4}$$

Equation (1) can be used to pursue integration of Eq. (3), with respect to v in order to deduce the internal energy e as a function of v and s,

$$e(v, s) = A\frac{v_0}{R_1} \exp\left(-R_1 \frac{v}{v_0}\right) + B\frac{v_0}{R_2} \exp\left(-R_2 \frac{v}{v_0}\right) + \frac{v_0 C(s)}{\Gamma} \left(\frac{v}{v_0}\right)^{-\Gamma} + E(s). \tag{5}$$

The unknown integration function $E(s)$ only depends on entropy and will be determined in the following. Similarly to Eq. (2), a reference energy curve $e_{\text{ref}}(v) = e(v, s_{\text{ref}})$ can be selected and written as,

$$e_{\text{ref}}(v) = A\frac{v_0}{R_1}\exp\left(-R_1\frac{v}{v_0}\right) + B\frac{v_0}{R_2}\exp\left(-R_2\frac{v}{v_0}\right) + \frac{v_0 C^*}{\Gamma}\left(\frac{v}{v_0}\right)^{-\Gamma} + E^*, \tag{6}$$

where $E^* = E(s_{\text{ref}})$ is a constant. Then Eqs. (5,6) are combined into a more convenient and compact form,

$$e(v, s) = e_{\text{ref}}(v) + \frac{v_0\left(C(s) - C^*\right)}{\Gamma}\left(\frac{v}{v_0}\right)^{-\Gamma} + E(s) - E^*. \tag{7}$$

At this point, it should be mentioned that in order to use this EOS, the functions $C(s)$ and $E(s)$ are yet to be determined. However, the EOS dependence with respect to entropy is not the preferred form of the JWL EOS. In typical numerical computations, the pressure needs to be computed at the end of a timestep from the specific volume and internal energy. Therefore, $p(v, e)$ form seems a more natural choice of EOS.

Additionally, the temperature T is a commonly used variable necessary for detailed chemistry models. Thus, the $p(v, T)$ form is also important. Therefore the following sections are devoted to the derivation of the various forms of the JWL model as a function of p, v, e, T, and other useful thermodynamic variables.

3. Mie-Grüneisen form

Mie-Grüneisen EOS is a family of widely used EOS (see *e.g.*, Ref.[26]), which exhibits a $p \propto e$ relation ensuring a simple numerical evaluation of the pressure during a numerical simulation. One of the advantageous features of the JWL model is that it can be recast in a Mie-Grüneisen form.

While a non-constant Grüneisen JWL model was proposed by [21], the constant Grüneisen assumption is the most commonly used in the literature. This work is restricted to the latter case. The Grüneisen function describes how temperature T responds to specific volume v changes [27] on an isentrope.

The Grüneisen coefficient Γ is defined by,

$$\Gamma = -\left(\frac{\partial \log T}{\partial \log v}\right)_s . \tag{8}$$

It can also be expressed by several thermodynamically equivalent forms including,

$$\Gamma = \frac{v}{T}\left(\frac{\partial p}{\partial s}\right)_v = v\left(\frac{\partial p}{\partial e}\right)_v = v\left(\frac{\partial p}{\partial s}\right)_v \left(\frac{\partial s}{\partial e}\right)_v . \tag{9}$$

A first important step towards the Mie-Grüneisen form of the JWL model is to notice that a constant Γ assumption actually places restrictions on the function $E(s)$. Indeed by injecting Eqs. (1,5) inside the last form of Eq. (9) leads to,

$$\Gamma = \frac{\Gamma \dfrac{dC}{ds}}{\dfrac{dC}{ds} + \dfrac{dE}{ds}\dfrac{\Gamma}{v_0}\left(\dfrac{v}{v_0}\right)^{\Gamma}} . \tag{10}$$

It is easily verified that this expression is only valid for a constant $E(s)$ function. This is a consequence of the constant Grüneisen assumption. Evaluation of this function on the reference isentrope characterized by s_{ref} yields,

$$E(s) = E^* . \tag{11}$$

Then thanks to the constant Grüneisen assumption, the second form of Eq. (9) can be integrated from the reference isentrope characterized by s_{ref} up to an arbitrary point, which state is defined by p, e, and v. Integration functions are therefore evaluated on the reference isentrope p_{ref} and e_{ref} given by Eqs. (2,6). This leads to the widely used Mie-Grüneisen form of the JWL EOS,

$$p(v,e) = p_{\text{ref}}(v) + \frac{\Gamma}{v}\left(e - e_{\text{ref}}(v)\right) . \tag{12}$$

Injection of the reference isentrope Eqs. (2,6) into Eq. (12) leads to an equivalent, less compact yet also interesting form,

$$\begin{aligned} p(v,e) = {} & \frac{\Gamma}{v}\left[e - E^*\right] \\ & + A\left(1 - \frac{v_0}{v}\frac{\Gamma}{R_1}\right)\exp\left(-R_1\frac{v}{v_0}\right) \\ & + B\left(1 - \frac{v_0}{v}\frac{\Gamma}{R_2}\right)\exp\left(-R_2\frac{v}{v_0}\right) . \end{aligned} \tag{13}$$

From this last expression, it is seen that C^* does not appear in the $p(v,e)$ form. It can also be seen that E^* effectively acts as the reference energy, which is used to introduce the heat of reaction in the products EOS.

Often used in high energy and high velocity problems the JWL square sound speed c^2 also needs to be computed along with the $p(v,e)$ EOS. It is expressed as a function of p, e, and v by,

$$c^2 = v^2 \left(\frac{\partial p}{\partial e}\right)_v \left(p + \left(\frac{\partial e}{\partial v}\right)_p\right). \tag{14}$$

These necessary partial derivatives are obtained from Eq. (13) and lead to,

$$\left(\frac{\partial p}{\partial e}\right)_v = \frac{\Gamma}{v}, \tag{15}$$

$$\begin{aligned}\left(\frac{\partial p}{\partial v}\right)_e = & -\frac{p}{v} \\ & + A\left(\frac{\Gamma+1}{v} - \frac{R_1}{v_0}\right)\exp\left(-R_1\frac{v}{v_0}\right) \\ & + B\left(\frac{\Gamma+1}{v} - \frac{R_2}{v_0}\right)\exp\left(-R_2\frac{v}{v_0}\right),\end{aligned} \tag{16}$$

$$\left(\frac{\partial e}{\partial v}\right)_p = -\left(\frac{\partial e}{\partial p}\right)_v \left(\frac{\partial p}{\partial v}\right)_e, \tag{17}$$

that can be injected inside Eq. (14). This yields the JWL sound speed expression as a function of p and v,

$$\begin{aligned}c^2(p,v) &= (\Gamma+1)\,pv \\ &- Av\left(\Gamma+1-\frac{R_1 v}{v_0}\right)\exp\left(-R_1\frac{v}{v_0}\right) \\ &- Bv\left(\Gamma+1-\frac{R_2 v}{v_0}\right)\exp\left(-R_2\frac{v}{v_0}\right).\end{aligned} \tag{18}$$

Elimination of the pressure also leads to the sound speed as a function of e

and v,

$$\begin{aligned} c^2(v,e) &= \Gamma\left(\Gamma+1\right)\left(e-E^*\right) \\ &+ A\left(\frac{v^2R_1}{v_0}-\frac{\Gamma\left(\Gamma+1\right)v_0}{R_1}\right)\exp\left(-R_1\frac{v}{v_0}\right) \\ &+ B\left(\frac{v^2R_2}{v_0}-\frac{\Gamma\left(\Gamma+1\right)v_0}{R_2}\right)\exp\left(-R_2\frac{v}{v_0}\right). \end{aligned} \tag{19}$$

With the $p(v,e)$ and sound speed $c^2(v,e)$ forms in hand, the JWL model can be used in a numerical code involving variables p, e, and v. The evaluation of the decomposition of the condensed explosive into gaseous products may request the determination of the temperature or the entropy, depending on the particular model [28]. Thus the thermal and caloric forms of the EOS are needed.

4. Thermal and Caloric forms

The previous section showed how the constant Grüneisen assumption allows to derive the useful $p(v,e)$ EOS from the $p(v,s)$ form. This section is dedicated to demonstrate that the assumption of a constant isochoric heat capacity defined by

$$C_v = \left(\frac{\partial e}{\partial T}\right)_v, \tag{20}$$

is sufficient to derive other forms of the JWL EOS as a function of enthalpy, entropy, and temperature.

The entropy total derivative with temperature T and specific volume v as independent variables is written as,

$$ds = \left(\frac{\partial s}{\partial v}\right)_T dv + \left(\frac{\partial s}{\partial T}\right)_v dT. \tag{21}$$

Then, standard thermodynamic definitions [25] can be used to express the following identities,

$$\left(\frac{\partial s}{\partial v}\right)_T = \frac{\Gamma C_v}{v}, \tag{22}$$

$$\left(\frac{\partial s}{\partial T}\right)_v = \frac{C_v}{T}. \tag{23}$$

Using constant-Γ and constant-C_v assumptions, Eqs. (22,23) are integrated and lead to,

$$s = \Gamma C_v \ln(v) + f_1(T) \,, \tag{24}$$

$$s = C_v \ln(T) + f_2(v) \,, \tag{25}$$

where $f_1(T)$ and $f_2(v)$ are functions of temperature and specific volume, respectively. Identification between those expressions and subtraction of the reference value s_{ref} lead to the $s(v,T)$ EOS,

$$\frac{s - s_{\text{ref}}}{C_v} = \ln\left(\frac{Tv^\Gamma}{\left[Tv^\Gamma\right]_{\text{ref}}}\right), \tag{26}$$

where $\left[Tv^\Gamma\right]_{\text{ref}}$ is a constant evaluated on the reference state characterized by $s = s_{\text{ref}}$. This form shows that Γ is directly related to isentropes in the T–v plane (see also Eq. (8)) and that Tv^Γ is constant along JWL isentropes. The Eq. (26) also leads to the $T(v,s)$ EOS,

$$T = v^{-\Gamma}\left[Tv^\Gamma\right]_{\text{ref}} \exp\left(\frac{s - s_{\text{ref}}}{C_v}\right). \tag{27}$$

Another total derivative, which is directly related to the $p(v,s)$ form Eq. (1) is introduced,

$$dp = \left(\frac{\partial p}{\partial v}\right)_s dv + \left(\frac{\partial p}{\partial s}\right)_v ds \,. \tag{28}$$

Standard thermodynamic definitions [25] can be used to express its partial derivatives as,

$$\left(\frac{\partial p}{\partial v}\right)_s = -\frac{c^2}{v^2}, \tag{29}$$

$$\left(\frac{\partial p}{\partial s}\right)_v = \frac{\Gamma T}{v} \,. \tag{30}$$

The Schwartz differentiability condition ensuring that p is a state function can be written as,

$$-\left(\frac{\partial}{\partial s}\left(\frac{c^2}{v^2}\right)\right)_v = \left(\frac{\partial}{\partial v}\left(\frac{\Gamma T}{v}\right)\right)_s , \tag{31}$$

which leads when combined with Eq. (27) to a first order differential equation,

$$\left(\frac{\partial}{\partial s}\left(c^2\right)\right)_v = \Gamma\left(\Gamma+1\right)\left[Tv^{\Gamma}\right]_{\mathrm{ref}} \exp\left(\frac{s-s_{\mathrm{ref}}}{C_v}\right) v^{-\Gamma}\,. \tag{32}$$

Then, Eq. (32) can be integrated between the reference state s_{ref} and an arbitrary value s,

$$\begin{aligned} c^2(v,s) &= c^2_{\mathrm{ref}}(v) \\ &\quad + \Gamma\left(\Gamma+1\right) C_v \left[Tv^{\Gamma}\right]_{\mathrm{ref}} \left(\exp\left(\frac{s-s_{\mathrm{ref}}}{C_v}\right)-1\right) v^{-\Gamma}\,, \end{aligned} \tag{33}$$

where $c^2_{\mathrm{ref}}(v) = c^2(v, s_{\mathrm{ref}})$ is the reference sound speed. This reference quantity is directly related to the reference isentrope by,

$$c^2_{\mathrm{ref}}(v) = -v^2\frac{dp_{\mathrm{ref}}}{dv} = v^2\frac{d^2 e_{\mathrm{ref}}}{dv^2}\,. \tag{34}$$

Equations (29,30) can be integrated with the help of Eqs. (27,33,34) and yield a system of two forms for $p(v,s)$ that should simultaneously be satisfied,

$$\begin{aligned} p(v,s) &= p_{\mathrm{ref}}(v) + f_3(s) \\ &\quad + \Gamma C_v \left[Tv^{\Gamma}\right]_{\mathrm{ref}} \left(\exp\left(\frac{s-s_{\mathrm{ref}}}{C_v}\right)-1\right) v^{-(\Gamma+1)}\,, \end{aligned} \tag{35}$$

$$p(v,s) = \Gamma C_v \left[Tv^{\Gamma}\right]_{\mathrm{ref}} \exp\left(\frac{s-s_{\mathrm{ref}}}{C_v}\right) v^{-(\Gamma+1)} + f_4(v)\,. \tag{36}$$

The functions $f_3(s)$ and $f_4(v)$ are evaluated by identifying the Eqs. (35) and (36) to each other and recalling that $p(v, s_{\mathrm{ref}}) = p_{\mathrm{ref}}(v)$. This finally yields the closed $p(v,s)$ form,

$$\begin{aligned} p(v,s) &= p_{\mathrm{ref}}(v) \\ &\quad + \frac{\Gamma C_v \left[Tv^{\Gamma}\right]_{\mathrm{ref}}}{v_0^{\Gamma}+1} \left(\exp\left(\frac{s-s_{\mathrm{ref}}}{C_v}\right)-1\right) \left(\frac{v}{v_0}\right)^{-(\Gamma+1)}\,. \end{aligned} \tag{37}$$

By using the reference JWL isentrope Eq. (2), one can also rewrite the $p(v,s)$ form as,

$$\begin{aligned} p(v,s) &= A\exp\left(-R_1\frac{v}{v_0}\right) + B\exp\left(-R_2\frac{v}{v_0}\right) + C^*\left(\frac{v}{v_0}\right)^{-(\Gamma+1)} \\ &\quad + \frac{\Gamma C_v \left[Tv^{\Gamma}\right]_{\mathrm{ref}}}{v_0^{\Gamma}+1} \left(\exp\left(\frac{s-s_{\mathrm{ref}}}{C_v}\right)-1\right) \left(\frac{v}{v_0}\right)^{-(\Gamma+1)}\,. \end{aligned} \tag{38}$$

This allows to finally identify the unknown function $C(s)$ from Eq. (1) as,

$$C(s) = \frac{\Gamma C_v \left[Tv^\Gamma\right]_{\text{ref}}}{v_0^\Gamma + 1} \left(\exp\left(\frac{s - s_{\text{ref}}}{C_v}\right) - 1\right) + C^* \,. \tag{39}$$

The Eq. (7) can be used to express the $e(v, s)$ EOS as,

$$e(v, s) = e_{\text{ref}}(v) + \frac{C_v \left[Tv^\Gamma\right]_{\text{ref}}}{v_0^\Gamma} \left(\exp\left(\frac{s - s_{\text{ref}}}{C_v}\right) - 1\right) \left(\frac{v}{v_0}\right)^{-\Gamma} \,. \tag{40}$$

Thanks to the $T(v, s)$ form, Eq. (27) $C(s)$ can also be expressed as a function of temperature and specific volume,

$$C(v, T) = \frac{\Gamma C_v T v^\Gamma}{v_0^\Gamma + 1} + K \,. \tag{41}$$

The new constant K , which practical influence will be highlighted later, is defined as,

$$K = C^* - \frac{\Gamma C_v \left[Tv^\Gamma\right]_{\text{ref}}}{v_0^\Gamma + 1} \,. \tag{42}$$

The thermal $p(v, T)$ form can be deduced from Eqs. (1,41) and reads as,

$$\begin{aligned} p(v, T) = \frac{\Gamma C_v T}{v} + K \left(\frac{v}{v_0}\right)^{-(\Gamma + 1)} \\ + A \exp\left(-R_1 \frac{v}{v_0}\right) + B \exp\left(-R_2 \frac{v}{v_0}\right) \,. \end{aligned} \tag{43}$$

The last three terms are found similar to the main isentrope $p_{\text{ref}}(v)$ except for constant C^* being replaced by K, this important detail being discussed in Appendix. The caloric $e(v, T)$ form is similarly deduced from Eqs. (5,11,41),

$$\begin{aligned} e(v, T) = C_v T + \frac{v_0 K}{\Gamma} \left(\frac{v}{v_0}\right)^{-\Gamma} + E^* \\ + A \frac{v_0}{R_1} \exp\left(-R_1 \frac{v}{v_0}\right) + B \frac{v_0}{R_2} \exp\left(-R_2 \frac{v}{v_0}\right) \,. \end{aligned} \tag{44}$$

Defining the specific enthalpy as $h = e + pv$, one is led to the $h(v,T)$ relation,

$$h(v,T) = (\Gamma+1)\,C_vT + Kv_0\left(\frac{1}{\Gamma}+1\right)\left(\frac{v}{v_0}\right)^{-\Gamma} + E^* + A\left(\frac{v_0}{R_1}+v\right)\exp\left(-R_1\frac{v}{v_0}\right) + B\left(\frac{v_0}{R_2}+v\right)\exp\left(-R_2\frac{v}{v_0}\right). \tag{45}$$

Additionally, the $c^2(v,T)$ form can also be obtained by elimination of pressure from Eqs. (18,43),

$$\begin{aligned} c^2(v,T) &= \Gamma\,(\Gamma+1)\,C_vT + (\Gamma+1)\,Kv_0\left(\frac{v}{v_0}\right)^{-\Gamma} \\ &+ A\frac{R_1v^2}{v_0}\exp\left(-R_1\frac{v}{v_0}\right) + B\frac{R_2v^2}{v_0}\exp\left(-R_2\frac{v}{v_0}\right). \end{aligned} \tag{46}$$

A last variable that is interesting to compute is Z the compressibility factor [29]. It scales with $\propto pv/T$ and its value is 1 in the ideal-gas limit where $v/v_0 \to \infty$ *i.e.* when v is sufficiently large to neglect attraction and repulsion between molecules. Hence it is expressed for the JWL as,

$$Z = \frac{pv}{\Gamma C_vT} = 1 + \frac{Kv_0}{\Gamma C_vT}\left(\frac{v}{v_0}\right)^{-\Gamma} + \frac{Av}{\Gamma C_vT}\exp\left(-R_1\frac{v}{v_0}\right) + \frac{Bv}{\Gamma C_vT}\exp\left(-R_2\frac{v}{v_0}\right). \tag{47}$$

In the ideal-gas limit, $Z = 1$ and the specific volume of the gas is $v_{\text{ig}} = \Gamma C_vT/p$. In the general case, $v = Zv_{\text{ig}}$. When $Z < 1$ (*resp.* $Z > 1$), the specific volume of the gas is smaller (*resp.* larger) than the corresponding ideal-gas with identical p and T indicating that attraction (*resp.* repulsion) effects between molecules are dominant. By inspecting the signs of the three terms $\propto K$, $\propto A$, and $\propto B$, it is possible to determine whether these terms are participating to attraction or repulsion effects when compared with the ideal-gas limit of the EOS.

5. Calibration to the Chapman-Jouguet state

Sets of reference data of a given explosive composition are used to calibrate the JWL coefficients (A, B, C^*, R_1, R_2, Γ, and v_0) of the main isentrope

Eq. (2), which is therefore completely characterized, see *e.g.*, Refs.[17, 30]. Alternatively, [20] proposed a methodology based on universal scalings for known explosive compositions to calibrate a JWL EOS by only using the initial explosive density $1/v_0$ and the CJ detonation velocity D_{CJ} as inputs. In the present study, it was chosen to follow a simple calibration guideline, based on the CJ state, see [18, 19]. This process is briefly summarized hereafter for completeness.

The reference isentrope $p_{\mathrm{ref}}(v)$ is chosen as the CJ isentrope, $p_{\mathrm{CJ}} = p_{\mathrm{ref}}(v_{\mathrm{CJ}})$. For an unreacted energetic material initially at standard conditions $p_0 = 101325$ Pa and $T_0 = 298.15$ K, the jump conditions across a CJ detonation characterized by v_{CJ}, $p_{\mathrm{CJ}} \gg p_0$, $e_{\mathrm{CJ}} \gg e_0$, and D_{CJ} lead to,

$$p_{\mathrm{CJ}} = \frac{D_{\mathrm{CJ}}^2}{v_0^2}\left(v_0 - v_{\mathrm{CJ}}\right) , \tag{48}$$

$$e_{\mathrm{CJ}} = \frac{p_{\mathrm{CJ}}}{2}\left(v_0 - v_{\mathrm{CJ}}\right) , \tag{49}$$

Additionally, the tangency of the isentrope with the Rayleigh line at the CJ point yields,

$$\frac{dp_{\mathrm{ref}}}{dv}\left(v = v_{\mathrm{CJ}}\right) = -\frac{D_{\mathrm{CJ}}^2}{v_0^2} . \tag{50}$$

It is worth mentioning that the thermodynamic identity $\gamma = -v\left(\partial p/\partial v\right)_s / p$ combined with Eq. (50) leads to,

$$\gamma_{\mathrm{CJ}} = \frac{D_{\mathrm{CJ}}^2}{v_0 p_{\mathrm{CJ}}} - 1 , \tag{51}$$

where γ_{CJ} is the adiabatic exponent at the CJ state. The Eqs. (48-50) are a set of three constraints that need to be met at the CJ point by the JWL EOS. Following [22], E^* is related to the heat of detonation $q > 0$ by $E^* \approx -q$. Using this result along with Eqs. (2,6,48-50) evaluated for $v = v_{\mathrm{CJ}}$ allows to express

a set of three relations between the CJ state and the JWL parameters,

$$p_{\mathrm{CJ}} = A\exp\left(-R_1\frac{v_{\mathrm{CJ}}}{v_0}\right) + B\exp\left(-R_2\frac{v_{\mathrm{CJ}}}{v_0}\right) + C^*\left(\frac{v_{\mathrm{CJ}}}{v_0}\right)^{-(\Gamma+1)}, \tag{52}$$

$$\frac{v_0 p_{\mathrm{CJ}}^2}{2D_{\mathrm{CJ}}^2} = \frac{A}{R_1}\exp\left(-R_1\frac{v_{\mathrm{CJ}}}{v_0}\right) + \frac{B}{R_2}\exp\left(-R_2\frac{v_{\mathrm{CJ}}}{v_0}\right) + \frac{C^*}{\Gamma}\left(\frac{v_{\mathrm{CJ}}}{v_0}\right)^{-\Gamma} - \frac{q}{v_0}, \tag{53}$$

$$\frac{D_{\mathrm{CJ}}^2}{v_0} = AR_1\exp\left(-R_1\frac{v_{\mathrm{CJ}}}{v_0}\right) + BR_2\exp\left(-R_2\frac{v_{\mathrm{CJ}}}{v_0}\right) + C^*(\Gamma+1)\left(\frac{v_{\mathrm{CJ}}}{v_0}\right)^{-(\Gamma+2)}. \tag{54}$$

This means that having calibrated 3 parameters among A, B, C^*, R_1, R_2, and Γ, the other ones are automatically deduced from Eqs. (52-54) by specifying the unreacted specific volume v_0 and its CJ state characterized by p_{CJ}, D_{CJ}, and q. Following [18, 19], the parameters A, B, and C^* can be expressed from R_1, R_2, Γ and the CJ state,

$$A = \exp\left(R_1\frac{v_{\mathrm{CJ}}}{v_0}\right)\frac{R_1}{R_1-R_2}\times \tag{55}$$
$$\frac{p_{\mathrm{CJ}}\left(1+\Gamma-\frac{R_2^2 v_{\mathrm{CJ}}^2}{\Gamma v_0^2}\right) - \left(\frac{v_0 p_{\mathrm{CJ}}^2}{2D_{\mathrm{CJ}}^2}+\frac{q}{v_0}\right)\left(1+\Gamma-\frac{R_2 v_{\mathrm{CJ}}}{v_0}\right)R_2 - \frac{D_{\mathrm{CJ}}^2 v_{\mathrm{CJ}}}{v_0^2}\left(1-\frac{R_2 v_{\mathrm{CJ}}}{\Gamma v_0}\right)}{1+\Gamma-(R_1+R_2)\frac{v_{\mathrm{CJ}}}{v_0}+\frac{R_1R_2v_{\mathrm{CJ}}^2}{\Gamma v_0^2}},$$

$$B = \exp\left(R_2\frac{v_{\mathrm{CJ}}}{v_0}\right)\frac{R_2}{R_2-R_1}\times \tag{56}$$
$$\frac{p_{\mathrm{CJ}}\left(1+\Gamma-\frac{R_1^2 v_{\mathrm{CJ}}^2}{\Gamma v_0^2}\right) - \left(\frac{v_0 p_{\mathrm{CJ}}^2}{2D_{\mathrm{CJ}}^2}+\frac{q}{v_0}\right)\left(1+\Gamma-\frac{R_1 v_{\mathrm{CJ}}}{v_0}\right)R_1 - \frac{D_{\mathrm{CJ}}^2 v_{\mathrm{CJ}}}{v_0^2}\left(1-\frac{R_1 v_{\mathrm{CJ}}}{\Gamma v_0}\right)}{1+\Gamma-(R_1+R_2)\frac{v_{\mathrm{CJ}}}{v_0}+\frac{R_1R_2v_{\mathrm{CJ}}^2}{\Gamma v_0^2}},$$

$$C^* = \frac{-p_{\mathrm{CJ}}(R_1+R_2) + \left(\frac{v_0 p_{\mathrm{CJ}}^2}{2D_{\mathrm{CJ}}^2}+\frac{q}{v_0}\right)R_1R_2 + \frac{D_{\mathrm{CJ}}^2}{v_0}}{1+\Gamma-(R_1+R_2)\frac{v_{\mathrm{CJ}}}{v_0}+\frac{R_1R_2v_{\mathrm{CJ}}^2}{\Gamma v_0^2}}\left(\frac{v_{\mathrm{CJ}}}{v_0}\right)^{(\Gamma+2)}. \tag{57}$$

$1/v_0$ ($\mathrm{kg/m^3}$)	p_{CJ} ($10^9\mathrm{Pa}$)	D_{CJ} ($\mathrm{m \cdot s^{-1}}$)	q ($10^6\mathrm{J \cdot kg^{-1}}$)	A ($10^9\mathrm{Pa}$)	B ($10^9\mathrm{Pa}$)	C^* ($10^9\mathrm{Pa}$)	R_1	R_2	Γ	C_v ($\mathrm{J \cdot kg^{-1} \cdot K^{-1}}$)	T_{CJ} (K)
1891	42.0	9110	5.552	773.98	11.18	0.6126	4.2	1.0	0.30	2800	3777

Table 1: Example of JWL parameters for HMX. v_0, p_{CJ}, D_{CJ}, q (corresponding to $E_0 v_0$ in [17]), R_1, R_2, and Γ are taken from [17]. A, B, and C are calculated from Eqs. (55-57). The remaining parameters C_v and T_{CJ} are estimated from the thermochemical code SIAME [31, 32].

Then, the constant K can be expressed from Eq. (42) and the fact that the reference isentrope passes through the CJ state,

$$K = C^* - \frac{\Gamma C_v T_{\mathrm{CJ}} v_{\mathrm{CJ}}^{\Gamma}}{v_0^{\Gamma} + 1} \,. \tag{58}$$

The Eqs. (55-58) show that the constants A, B, and C^* are uniquely defined by the CJ state, Γ, R_1, and R_2. The literature is abundant for the latter parameters, see *e.g.* [17, 20]. However, the constant K needs an additional estimate for $C_v T_{\mathrm{CJ}}$, which is more difficult to find. Reasonable estimates are provided by the thermochemical code SIAME [31, 32]. Table 1 summarizes a set of calibrated parameters for HMX that will be used hereafter to study the validity domain of the JWL model.

The calibrated main isentrope $p_{\mathrm{ref}}(v)$ is illustrated in Fig. 1 along with the relative proportion of the three terms proportional to A, B, and C^*, respectively. Three regions can be distinguished.

- Close to the CJ state, the first exponential term $\propto A$ represents more than 80% of the main isentrope. This highlights the importance of the exponential term in the modeling of the CJ state.

- For a pressure of the order of 0.1% of p_{CJ} (this threshold value is 42 MPa for HMX) and below, the exponential terms are completely negligible and the main isentrope is of the ideal-gas form $p_{\mathrm{ref}}(v) \propto v^{-(\Gamma+1)}$.

- Between those two regions, the second exponential term $\propto B$ exhibits a local maximum of more than 80% allowing a smooth transition between the first exponential term and the ideal-gas term of the main isentrope.

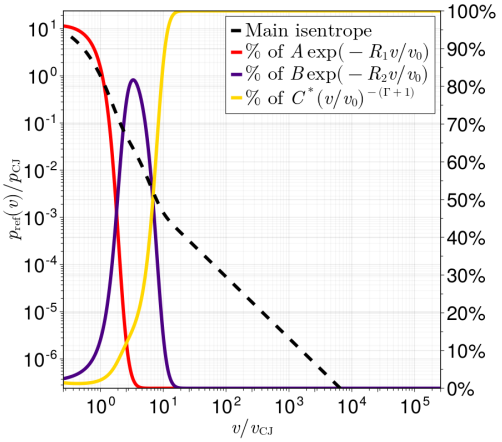

Figure 1: Main isentrope $p_{\mathrm{ref}}(v)$ JWL for HMX. The relative proportion of each terms is measured in % on the right axis.

Other isentropes in the p–v plane are shown in Fig. 2. The observed region without isentropes for small v corresponds to a negative temperature $T < 0$ region in which the entropy s does not admits any real solution. It can be seen that isentropes are extremely close to each other near the CJ state but tend to drift apart during an expansion process. This means that when modeling detonation products undergoing a subsequent expansion to atmospheric pressure, an initial few percent departure from the CJ state could eventually lead to a much larger departure after expansion. This effect is easily noticeable for isentropes going through a state with both $p < p_{\mathrm{CJ}}$ and $v < v_{\mathrm{CJ}}$. One can also notice that isentropes are actually straight lines (in the logarithmic scale) in a large portion of the domain corresponding to regions where the exponential terms are negligible and where the isentropes essentially behave as ideal-gas ones, $p \propto v^{-(\Gamma+1)}$.

The adiabatic exponent characterizing p–v isentropes is expressed by,

$$\gamma = -\frac{v}{p}\left(\frac{\partial p}{\partial v}\right)_s = -\left(\frac{\partial \log p}{\partial \log v}\right)_s = \frac{c^2}{pv}\,. \tag{59}$$

Its evolution along the CJ isentrope can also be found in Figure 3 and shows that $\gamma(v_{\mathrm{CJ}}) \approx 2.74$ while expanded gases reach a plateau $\gamma = \Gamma + 1 = 1.3$ for roughly $v > 10\, v_{\mathrm{CJ}}$. The curve also exhibits a double maxima, which is classical of JWL EOS [6]. For isentropic compressions from the CJ state, the adiabatic exponent rapidly drops below 1.

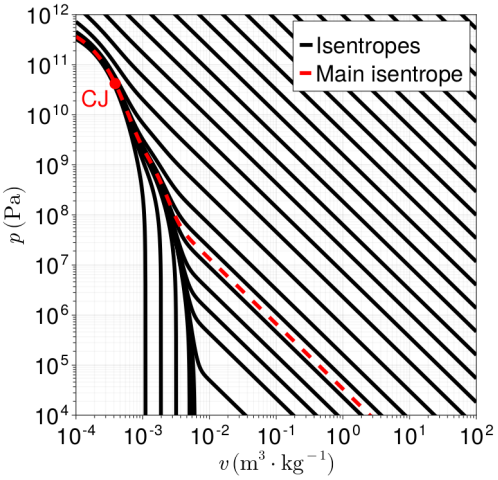

Figure 2: JWL isentropes for HMX in the p–v plane.

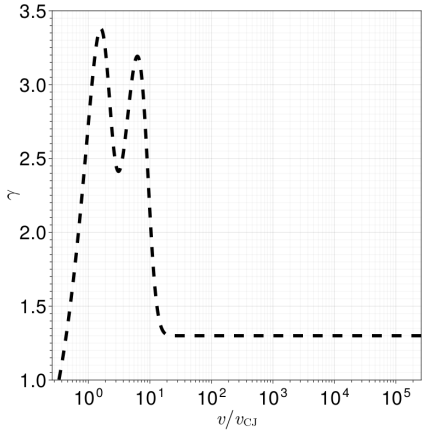

Figure 3: Adiabatic exponent γ along the CJ isentrope versus the ratio of specific volume.

6. Domain of validity in p–v and T–v planes

In order for the JWL model to remain physically consistent, a set of constraints should be verified at least in a bounded domain, deemed as the domain of validity in which the EOS can be safely used in hydrocodes.

A common constraint is the positivity of the square sound speed $c^2 \geq 0$ that allows the model to remain hyperbolic, but other conditions related to the thermodynamic stability and to the Riemann problem can also be found in the literature [33–36]. The following constraints are expected to hold in the domain of validity of the EOS.

- 1) The resulting Euler system governing a JWL material is hyperbolic as long as these conditions hold true,

$$c^2 \geq 0\,, \quad \left(\frac{\partial^2 p}{\partial v^2}\right)_s \geq 0\,. \tag{60}$$

  The square of the sound speed is positive and the isentropes are convex in the p–v plane. The latter condition can also be related to the positivity of the fundamental derivative [34]. It should be mentioned that the loss of convexity is often related to the non-analytic behavior of an EOS due to phase transitions and does not necessarily correspond to an unphysical behavior. For the remainder of the article, the Eqs. (60) will be referred to as the convexity criteria.

- 2) Owing to physical or numerical noise, a system is always subject to perturbations. Assuming that it is in thermodynamic equilibrium, this system exhibits a maximum entropy and must remain stable in face of perturbations leading to a decrease of entropy. The stability of the thermodynamic equilibrium requires the internal energy to be convex, as respect to the specific volume v and the entropy s. These conditions translate to the following inequalities Eq. (61),

$$\gamma = \frac{c^2}{pv} \geq 0\,, \quad g = \frac{pv}{C_v T} \geq 0\,, \quad \gamma g \geq \Gamma^2\,, \tag{61}$$

  where γ is the classical adiabatic exponent, which acts as a dimensionless sound speed and g is a reciprocal dimensionless heat capacity scaling directly with the compressibility factor [37].

- 3) An initial value problem, which initial condition is made of two domains with constant fields separated by a discontinuity is known as the Riemann problem. The Riemann problem can be considered as the hallmark of shock physics. Detonation products modeled by a JWL material are likely to be subjected to reflected secondary shocks for which the Riemann problem is expected to produce physically consistent waves, *e.g.* compression across shocks and expansion across rarefaction waves. This is ensured if v^{-1}, e, u (material velocity), and p are monotonically increasing along the Hugoniot curve in the direction of increasing shock strength. According to [34] this translates into the weak (Eq. (62a)), medium (Eq. (62b)) and strong conditions (Eq. (62c)),

$$(a) \quad 2\gamma \geq \Gamma, (b) \quad \frac{pv}{2e} + \gamma \geq \Gamma, (c) \quad \frac{pv}{e} \geq \Gamma. \tag{62}$$

  When $\left(\partial^2 p/\partial v^2\right)_s \geq 0$, both weak and medium conditions can be derived from the strong condition. The simultaneous validity of the convexity criteria Eqs. (60) and the weak condition is referred to as Bethe-Weyl theorem.

Based on the HMX calibration parameters from Table 1, it is possible to study the domain of validity in which constraints the Eqs. (60-62) are valid. Although other explosive compositions have different sets of parameters, the present discussion is merely designed to highlight qualitative trends of the JWL model that have also been observed when calibrated with other explosives, *e.g.* PBX9501 [15] or TNT [14].

6.1. Pressure and temperature positivity

The positivity of T in the p–v plane is investigated in Fig. 4. The blank region corresponds to the negative temperature $T < 0$ portion of the domain showing that lower specific volumes than approximately 10^{-3} $\mathrm{m}^3{\cdot}\mathrm{kg}^{-1}$ lead to a negative temperature in the range from the atmospheric pressure to the CJ pressure. This excludes a large portion of the domain of validity of the EOS in which the entropy does not admit a real value. This region is due to the large positive coefficients A and B in Eq. (43) modeling the repulsive effects between molecules in a dense gas.

Examination of the main isentrope represented as a dashed line shows that it closely runs along the boundary of the $T \geq 0$ region in the vicinity of the CJ

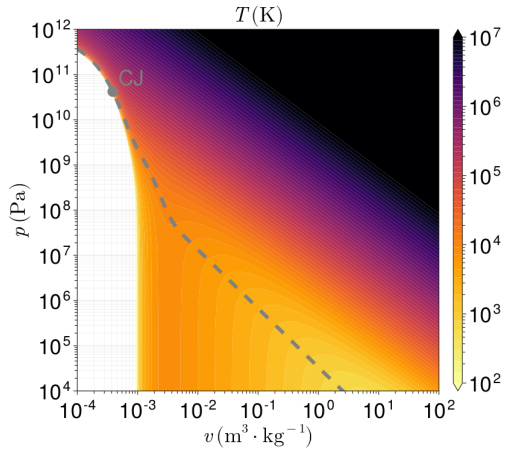

Figure 4: $T \geq 0$ domain in the p–v plane for HMX. The dashed line corresponds to the main isentrope and blank regions to $T < 0$.

point. This indicates that non-isentropic transformations or numerical errors in a detonated CJ state could easily induce a drift of the thermodynamic state inside the $T < 0$ region.

A similar investigation is carried out in the T–v plane in order to highlight $p \geq 0$ regions. It should be mentioned that all isentropes are straight lines (in logarithmic scale) in this plane due to the constant Grüneisen parameter Γ. Figure 5 shows that a large portion of specific volumes larger than approximately 10^{-3} $\mathrm{m}^3{\cdot}\mathrm{kg}^{-1}$ and below the main isentrope leads to a negative pressure. This even excludes some low temperatures encountered in atmospheric conditions and shows that the JWL EOS is not meant to model low temperatures. In Eq. (43), this $p < 0$ region is due to the negative and large coefficient K obtained from the calibration summarized in Table 1 and effectively modeling attraction between molecules (see Eq. (47)), which leads to $Z < 1$ for sufficiently low T.

6.2. Convexity, positivity of the square sound speed

The map of validity of the convexity criteria (see Eqs. (60)) colored by the sound speed can be found on Fig. 6 and 7 for the p–v and T–v planes, respectively.

In the blank region in Fig. 6, pressure is negligible in front of A and B such that $(\Gamma + 1)/R_1$ and $(\Gamma + 1)/R_2$ being larger than v/v_0 tend to promote the appearance of a non-convexity region (see Eq. (17)).

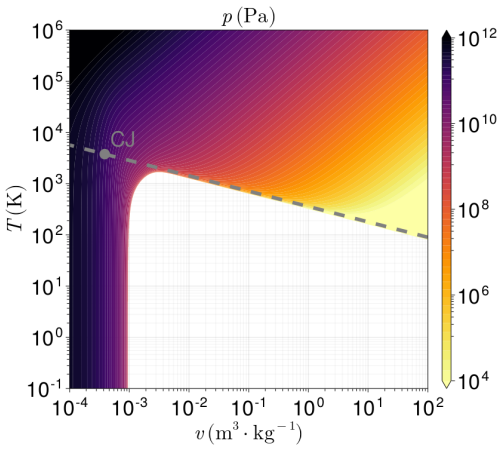

Figure 5: $p \geq 0$ domain in the T–v plane for HMX. The dashed line corresponds to the main isentrope and blank regions to $p < 0$.

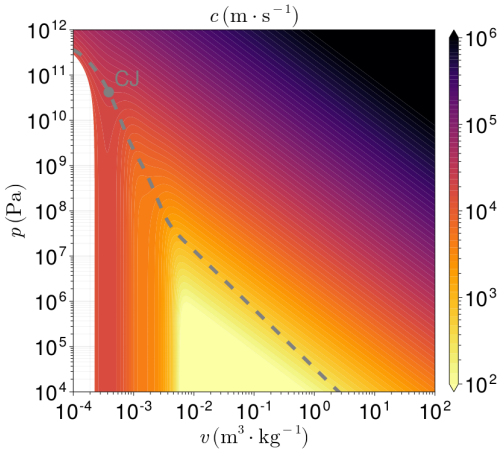

Figure 6: Convexity domain colored by c in the p–v plane for HMX. The dashed line corresponds to the main isentrope and blank regions to the violation of the convexity criteria, *i.e.* $c^2 < 0$ and/or $(\partial^2 p/\partial v^2)_s < 0$.

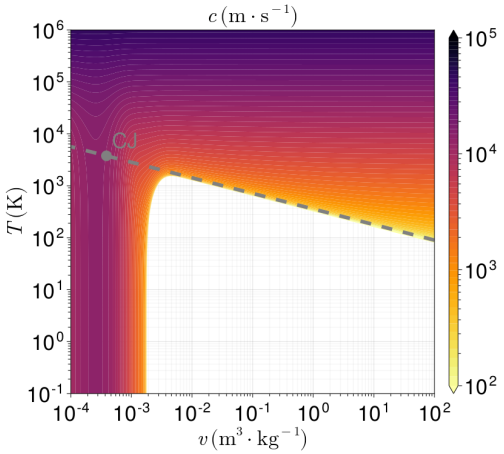

Figure 7: Convexity domain colored by c in the T–v plane for HMX. The dashed line corresponds to the main isentrope and blank regions to the violation of the convexity criteria, *i.e.* $c^2 < 0$ and/or $(\partial^2 p/\partial v^2)_s < 0$.

The blank region in Fig. 7 is due to the large negative value K dominating the exponential terms at low temperatures and sufficiently large specific volumes. Therefore, it is found that convexity criteria ($c^2 \geq 0$ and $(\partial^2 p/\partial v^2)_s \geq 0$, Eqs. (60)) are less restrictive than the conditions $T \geq 0$ and $p \geq 0$ in order to delineate the p–v and T–v domains of validity.

6.3. Stability of thermodynamic equilibrium with respect to fluctuations

Contrarily to the convexity criteria Eqs. (60), the thermodynamic stability conditions Eqs. (61) introduce qualitatively different restrictions in the validity domain. The thermodynamic stability region in the p–v plane colored by $g = pv/(C_v T)$ can be found on Fig. 8.

It shows two different unstable regions. The first one is equivalent to the $T < 0$ region previously described and is also controlled by the large positive A and B meant to model short distance repulsion in a dense gas. Indeed, the compressibility factor Z (Eq. (47)) is composed of three terms, of which sign depends on K, A, and B. $K < 0$ represents attraction, $A > 0$ and $B > 0$ repulsion between molecules. And here the terms proportional to A and B tend towards 0 faster than the term proportional to K when the specific volume v is very high when compared to v_0.
However, a second and qualitatively different blank region is present and shows that thermodynamic stability is also violated in a low pressure portion

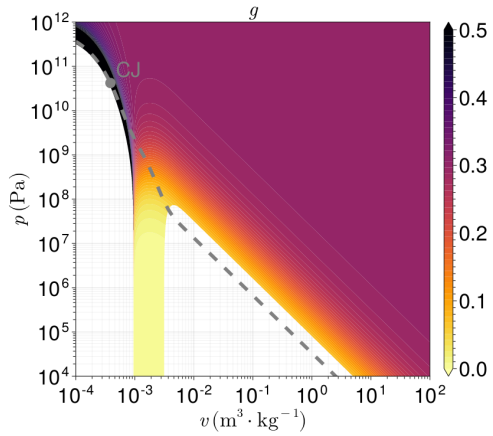

Figure 8: Domain for the stability of thermodynamic equilibrium in the p–v plane for HMX. The dashed line corresponds to the main isentrope and blank regions either to thermal or mechanical unstable states, *i.e.* $\gamma < 0$ and/or $g < 0$ and/or $\gamma g < \Gamma^2$.

mainly below the main isentrope. A comparison with Fig. 2 shows that expansions following isentropes below the CJ isentrope can easily reach this region. This is a well known problem of the JWL EOS [22]. Indeed, varying the $C_v T_{\mathrm{CJ}}$ parameter will shift the unstable regions regardless of the value of the main isentrope, which is independent of $C_v T_{\mathrm{CJ}}$. This highlights the difficulties of the JWL EOS close to atmospheric conditions.

Assuming that previous conditions (positive p, T and c^2) are verified, the stable thermodynamic equilibrium conditions Eqs. (61) reduce to $C_v \geq 0$ and $c^2/(C_v T) \geq \Gamma^2$. The former being automatically enforced by the input parameters, the origin of the qualitatively new blank region can be explained by studying the value of $c^2/(C_v T)$ which is always larger than Γ^2 except when the negative term scaling with K dominates (see Eq. (46)).

Perhaps the less intuitive result from Fig. 8 is that the expansion isentrope from the CJ state reaches the region of unstable thermodynamic equilibrium long before reaching the atmospheric pressure, at roughly 10^8Pa for the present HMX calibration.

The equivalent T–v domain of stable thermodynamic equilibrium can be found on Fig. 9 and only shows slight but sufficient differences with respect to previous conditions such that the T–v isentrope is reaching the unstable thermodynamic equilibrium region long before reaching atmospheric temperatures.

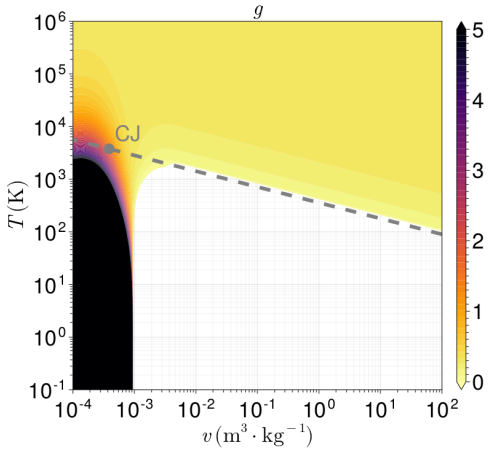

Figure 9: Domain for the stability of thermodynamic equilibrium in the T–v plane for HMX. The dashed line corresponds to the main isentrope and blank regions either to thermal or mechanical unstable states, *i.e.* $\gamma < 0$ and/or $g < 0$ and/or $\gamma g < \Gamma^2$.

6.4. Bethe-Weyl theorem and monotonicity along the Hugoniot curve

In order to ensure existence and uniqueness of the shock solution to the Riemann problem, the Bethe-Weyl theorem should be verified. It combines the convexity criterion Eqs. (60) with the weak condition from Eqs. (62). The domain of validity of this theorem is investigated in Figs. 10 and 11 for the p–v and T–v planes, respectively.

It can be seen that this theorem is actually less restrictive than the positive pressure and temperature conditions.

However the Bethe-Weyl theorem does not ensures the monotonicity of all thermodynamic fields along the Hugoniot curve [34]. A more stringent constraint ensuring monotonicity along the Hugoniot is the strong condition Eqs. (62c). The domain of validity of this constraint is highlighted in the p–v and T–v planes and colored by e in Figs. 12 and 13, respectively.

It is found that this condition excludes larger portions in the p–v and T–v planes while maintaining the same qualitative behavior than the $p \geq 0$ and $T \geq 0$ conditions.

7. Conclusion

A standalone derivation and investigation of the JWL EOS is proposed. The step-by-step demonstration entirely stems from three necessary assump-

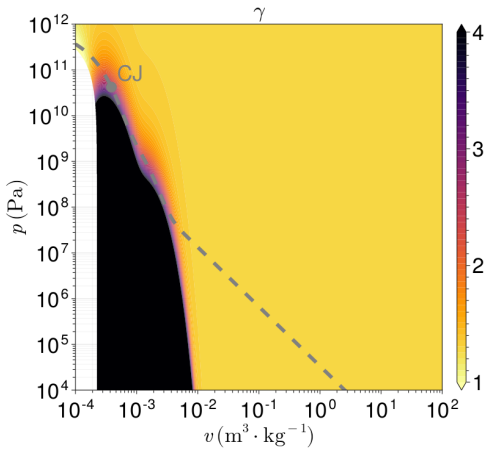

Figure 10: Bethe-Weyl p–v domain colored by γ for HMX. The dashed line corresponds to the main isentrope and blank regions to violation of the Bethe-Weyl theorem, *i.e.* $c^2 < 0$ and/or $(\partial^2 p/\partial v^2)_s < 0$ and/or $2\gamma < \Gamma$.

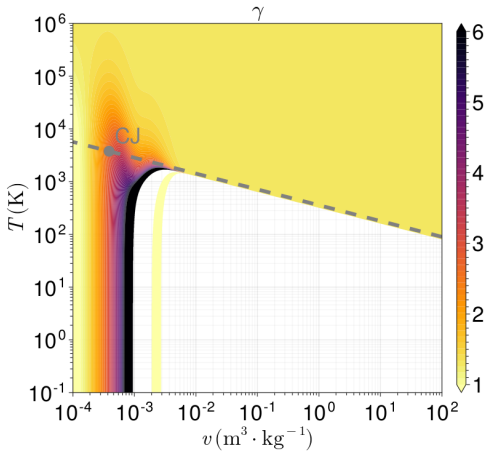

Figure 11: Bethe-Weyl T–v domain colored by γ for HMX. The dashed line corresponds to the main isentrope and blank regions to violation of the Bethe-Weyl theorem, *i.e.* $c^2 < 0$ and/or $(\partial^2 p/\partial v^2)_s < 0$ and/or $2\gamma < \Gamma$.

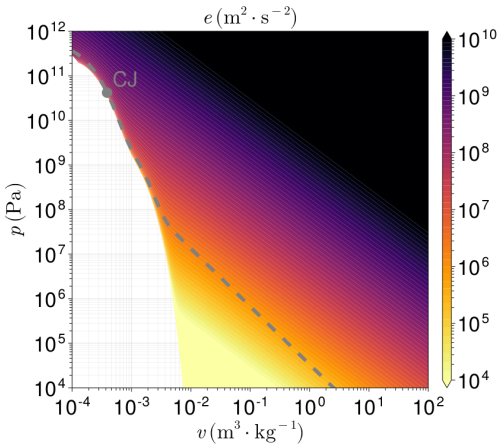

Figure 12: Strong condition in the p–v domain colored by e for HMX. The dashed line corresponds to the main isentrope and blank regions to an ill-posed Riemann problem, *i.e.* $pv/e < \Gamma$.

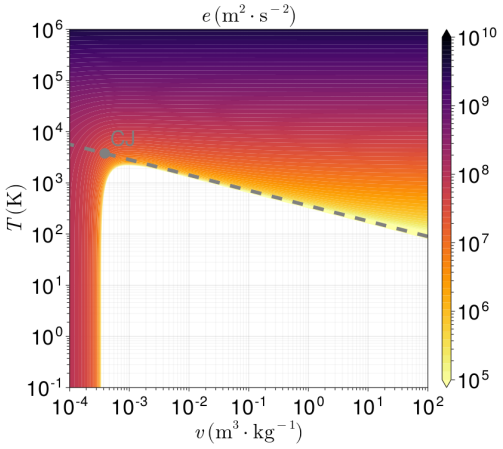

Figure 13: Strong condition in the T–v domain colored by e for HMX. The dashed line corresponds to the main isentrope and blank regions to an ill-posed Riemann problem, *i.e.* $pv/e < \Gamma$.

tions to fully describe the JWL EOS: the main isentrope $p_{\text{ref}}(v)$ is known, both Grüneisen Γ and isochoric heat capacity C_v are constant. Alternatively, the JWL model could be entirely derived from a complete form of the EOS – usually $e(v, s)$ – see *e.g.* [34] for more details. The derivation of the other thermodynamic fields is explained and shows how each variable is modeled by the JWL EOS.

Then the usual choice of a reference isentrope passing through the CJ state of detonation products of HMX was selected for calibration. The relative importance of the various terms along the CJ isentrope is investigated, showing that exponential terms dominate in a narrow region around the CJ state and that CJ isentrope reduces to an ideal-gas below a threshold value of $p \approx 42\,\text{MPa}$. The various necessary thermodynamic constraints, which are positivity, convexity, stability and monotonicity along an Hugoniot are investigated in both the p–v and T–v planes and allows to identify and understand the different trends and limitations of the JWL model. Overall the JWL EOS is found to accurately reproduce CJ state due to its careful calibration.

However, this EOS lacks some flexibility for three cases that could be encountered in practical applications. First, it was seen that an isentropic compression from the CJ point lead to a significant reduction of the adiabatic exponent below 1. Second, the CJ isentrope typically reaches atmospheric conditions in the region of unstable thermodynamic equilibrium of both p–v and T–v diagrams. Third, low temperatures close to atmospheric conditions are usually outside of the domain of validity of the EOS.

These are not necessarily a problem for practical engineering applications because the EOS is interfaced with other models that could mitigate or delay the appearance of the mentioned anomalous behaviors due to violation of constraints Eqs. (60-62). However, one needs to keep in mind that these constraints exist and could possibly create artifacts and/or misinterpretations of physical phenomena.

Besides providing a step-by-step derivation of the main thermodynamic fields and increasing the understanding of the widely used JWL model, the present study also helps in identifying the properties of thermodynamic states with large departures from the CJ point that are likely to lie outside of the validity domain of this EOS.

Declaration of Competing Interest

The authors declare that they have no known competing financial interests or personal relationships that could have appeared to influence the work reported in this paper.

Acknowledgements

This work was supported by CEA Le Ripault.

Appendix A. Auxiliary functions $p_K(v)$ and $e_K(v)$

A careful examination shows that both $p(v,T)$ and $e(v,T)$ forms Eqs. (43,44) could also be written as,

$$p(v,T) = p_K(v) + \frac{\Gamma C_v T}{v}\,, \tag{A.1}$$

$$e(v,T) = e_K(v) + C_v T\,, \tag{A.2}$$

where functions $p_K(v)$ and $e_K(v)$ are related to the reference isentrope by,

$$p_K(v) = p_{\text{ref}}(v) + (K - C^*)\left(\frac{v}{v_0}\right)^{-(\Gamma+1)}\,, \tag{A.3}$$

$$e_K(v) = e_{\text{ref}}(v) + \frac{v_0}{\Gamma}(K - C^*)\left(\frac{v}{v_0}\right)^{-\Gamma}\,. \tag{A.4}$$

By noticing that the constant C^* vanishes from Eq. (13) it is possible to artificially rewrite the Mie-Grüneisen form $p(v,e)$ as,

$$p(v,e) = p_K(v) + \frac{\Gamma}{v}\left(e - e_K(v)\right)\,. \tag{A.5}$$

This shorthand is often used in the literature such that EOS forms involving p, v, e, and T only use one set of functions $p_K(v)$ and $e_K(v)$ rather than also having to use $p_{\text{ref}}(v)$ and $e_{\text{ref}}(v)$ in the Mie-Grüneisen form. Hence one should keep in mind that $p_K(v)$ and $e_K(v)$ are merely auxiliary functions meant to simplify the implementation of the JWL model and should not be misinterpreted as being the reference isentrope curve.

References

[1] M. R. Baer, J. W. Nunziato, *Int. J. Multiphas. Flow* **1986**, *12*, 861–889.

[2] F. Petitpas, R. Saurel, E. Franquet, A. Chinnayya, *Shock Waves* **2009**, *19*, 377–401.

[3] G. Baudin, A. Lefrancois, R. Saurel, F. Petitpas, O. L. Metayer, J. Massoni, V. M. Belski, E. Zotov, *J. Energ. Mater.* **2010**, *28*, 154–179.

[4] P. Vidal, E. Bouton, L. Pagnanini, *Combust. Flame* **2012**, *159*, 396–408.

[5] J. Kury, H. Hornig, E. Lee, J. McDonnel, D. Ornellas, M. Finger, F. Strange, M. Wilkins, *4th Symposium (International) on Detonation* **1965**, 3–13.

[6] E. Lee, H. Hornig, J. Kury, Adiabatic expansion of high explosive detonation products, tech. rep., No. TID 4500-UCRL 50422, Lawrence Livermore National Laboratory, University of California, Livermore, CA, USA, **1968**.

[7] H. Jones, A. Miller, *Proceedings of the Royal Society of London. Series A. Mathematical and Physical Sciences* **1948**, *194*, 480–507.

[8] M. L. Wilkins, B. Squier, B. Halperin, *Symp. (Int.) Combust.* **1965**, *10*, 769–778.

[9] O. Heuzé, *Phys. Rev. A* **1986**, *34*, 428.

[10] M. Hobbs, M. Baer, *Shock Waves* **1992**, *2*, 177–187.

[11] C. L. Mader, *Numerical modeling of explosives and propellants*, CRC press, **2007**.

[12] A. Chinnayya, E. Daniel, R. Saurel, *J. Comp. Phys.* **2004**, *196*, 490–538.

[13] J. Massoni, R. Saurel, A. Lefrancois, G. Baudin, *Shock Waves* **2006**, *16*, 75–92.

[14] E. Del Prete, A. Chinnayya, L. Domergue, A. Hadjadj, J.-F. Haas, *Shock Waves* **2013**, *23*, 39–53.

[15] R. Saurel, F. Fraysse, D. Furfaro, E. Lapebie, *Comput. Fluids* **2018**, *169*, 213–229.

[16] G. I. Taylor, *The scientific papers of GI Taylor* **1963**, *3*, 277–286.

[17] B. Dobratz, P. Crawford, LLNL Explosives Handbook, tech. rep., No. UCRL-52997, Lawrence Livermore National Laboratory, **1985**.

[18] P. Urtiew, B. Hayes, *Combust. Explos. Shock Waves* **1991**, *27*, 505–514.

[19] R. Trębiński, W. Trzciński, *Journal of Technical Physics* **1999**, *40*, 447–456.

[20] S. I. Jackson, *Combust. Flame* **2018**, *190*, 240–251.

[21] G. Baudin, R. Serradeill in EPJ Web of Conferences, *Vol. 10*, EDP Sciences, **2010**, p. 00021.

[22] R. Menikoff, JWL equation of state, tech. rep., No. LA-UR-15-29536, Los Alamos National Lab.(LANL), Los Alamos, NM (United States), **2015**.

[23] S. B. Segletes, An Examination of the JWL Equation of State, tech. rep., Weapons and Materials Research Directorate, US Army Research Laboratory, ARL, **2018**.

[24] P. W. Cooper, *9th Symposium (International) on Detonation* **1989**.

[25] J. H. Lee, K. Ramamurthi, *Fundamentals of thermodynamics*, CRC Press, **2022**.

[26] R. Menikoff, Complete Mie–Gruneisen equation of state (update), tech. rep., No. LA-UR-16-21706, Los Alamos National Lab.(LANL), Los Alamos, NM (United States), **2016**.

[27] S. Chandrasekhar, *An introduction to the study of stellar structure*, *Vol. 2*, Courier Corporation, **1957**.

[28] C. Handley, B. Lambourn, N. Whitworth, H. James, W. Belfield, *Appl. Phys. Rev.* **2018**, *5*, 011303.

[29] J. Smith, H. Van Ness, M. Abbott, M. Swihart, *Introduction to Chemical Engineering Thermodynamics, 9th Edition*, McGraw Hill Education, **2022**.

[30] S. Sheffield, R. Engelke, *Shock Wave Science and Technology Reference Library* **2009**, *3*.

[31] S. Poeuf, PhD thesis, ISAE-ENSMA Ecole Nationale Supérieure de Mécanique et d'Aérotechique-Poitiers, **2018**.

[32] S. Poeuf, M. Genetier, A. Lefrançois, A. Osmont, G. Baudin, A. Chinnayya, *Propell. Explos. Pyrot.* **2018**, *43*, 1157–1163.

[33] H. A. Bethe, *Classic papers in shock compression science* **1998**, 421–495.

[34] R. Menikoff, B. J. Plohr, *Rev. Mod. Phys.* **1989**, *61*, 75.

[35] G. Ben-Dor, O. Igra, T. Elperin, *Handbook of shock waves, three volume set*, Elsevier, **2000**.

[36] D. K. Kondepudi et al., *Introduction to modern thermodynamics*, *Vol. 666*, Wiley Chichester, **2008**.

[37] B. E. Poling, J. M. Prausnitz, J. P. O'connell, *Properties of gases and liquids*, McGraw-Hill Education, **2001**.